



Performance analysis of two generations of heaving point absorber WECs in farms of hexagon-shaped array layouts

Xinyuan Shao, Hua-Dong Yao, Jonas W. Ringsberg, Zhiyuan Li & Erland Johnson

To cite this article: Xinyuan Shao, Hua-Dong Yao, Jonas W. Ringsberg, Zhiyuan Li & Erland Johnson (13 Feb 2024): Performance analysis of two generations of heaving point absorber WECs in farms of hexagon-shaped array layouts, *Ships and Offshore Structures*, DOI: [10.1080/17445302.2024.2317658](https://doi.org/10.1080/17445302.2024.2317658)

To link to this article: <https://doi.org/10.1080/17445302.2024.2317658>



© 2024 The Author(s). Published by Informa UK Limited, trading as Taylor & Francis Group



Published online: 13 Feb 2024.



Submit your article to this journal [↗](#)



Article views: 359



View related articles [↗](#)



View Crossmark data [↗](#)

Performance analysis of two generations of heaving point absorber WECs in farms of hexagon-shaped array layouts

Xinyuan Shao^a, Hua-Dong Yao^a, Jonas W. Ringsberg ^a, Zhiyuan Li^a and Erland Johnson^{a,b}

^aDepartment of Mechanics and Maritime Sciences, Division of Marine Technology, Chalmers University of Technology, Gothenburg, Sweden;

^bDepartment of Applied Mechanics, RISE Research Institutes of Sweden, Borås, Sweden

ABSTRACT

Numerical analyses are presented for two generations of a floating heaving point absorber wave energy converter (WEC) installed with different farm array layouts. The wave farm configurations are based on WECs developed by Waves4Power. The numerical models are developed in the DNV software package, Sesam. Parametric studies of the isolated WEC configurations and farm array layouts are conducted under typical environmental conditions and various incident wave directions to understand the hydrodynamic power performance and the levelised cost of energy (LCoE). Hexagonal layouts are proposed for deploying the WEC units and compared with a 10-unit layout termed StarBuoy, which has been reported in previous work. The results of the present study confirm that the interactions between arrayed units in a farm can have either positive or negative effects on the LCoE, which is dependent on the array layout and environmental conditions. The hexagonal array layouts lead to lower LCoE owing to constructive interaction effects.

ARTICLE HISTORY

Received 8 December 2022
Accepted 8 January 2024

KEYWORDS

Array layout; environmental conditions; hexagon-shaped; interaction effects; levelised cost of energy; wave energy

Nomenclature



A	Wave amplitude [m]
B_{PTO}	Linear damping of power take-off system [-]
BEM	Boundary element method
CFD	Computational fluid dynamics
COG	Centre of gravity
FEM	Finite element method
I_p	Power interaction factor [-]
LCA	Life-cycle analysis
LCC	Life-cycle cost
LCoE	Levelised cost of energy
P	Power generation [W]
PTO	Power take-off
T	Wave period [s]
T_{sim}	Simulation time [s]
WEC	Wave energy converter
ξ	Heave motion [m]
6-degree-of-freedom	6-DOF

1. Introduction

Ocean wave energy has attracted attention as an essential complement to wind and solar energy sources because of its high energy density and persistence (Falnes 2007). Despite the advantages and large reserves, several obstacles still hinder the commercialisation of devices that extract energy from waves, known as wave energy converters (WEC). Unlike wind turbines and solar panels, which have generally accepted and optimised configurations, there is a large variety of WEC configurations that are categorised based on their working principles, including the oscillating water column, oscillating body, and overtopping devices (Falcao 2010). The diversity of WEC prototypes adds uncertainties to the technology development and performance evaluation because conclusions made for one WEC may not apply to another, indicating that WEC prototypes should be investigated on a case-by-case basis. Additionally,

the levelised cost of energy (LCoE) must be reduced to meet commercial requirements. The most common and intuitive way to achieve this is to deploy multiple WEC units in a single farm, or park, which can lower the cost by sharing anchors, moorings, and cables (Child and Venugopal 2010; Babarit 2013; Giassi 2020). However, the effects of hydrodynamic interactions, which are caused by radiation and diffraction between units, are shown to have constructive or destructive impacts on the power performance of WECs, according to analytical solutions (Budal 1977; Falnes 1980), experiments (Stallard et al. 2008; Weller et al. 2010) and numerical simulations (Babarit 2010; Borgarino et al. 2012; Engström et al. 2013; Lee et al. 2018). Moreover, numerous factors affect the interactions, for example, distances between deployed units, wave farm layouts, environmental conditions, incident wave directions, etc. (Götteman et al. 2014). Therefore, to lower the LCoE, the layout of a wave farm should be carefully designed to maximise constructive interactions while minimising destructive interactions under varied environmental conditions. However, different WEC configurations or concepts also impose different requirements on the layout.

Designing wave farm layouts is a complex task that covers several levels from preliminary to detailed design. For the preliminary design, it is necessary to determine some promising wave farm layouts with varying environmental parameters and under given constraints. Optimisation methods can be used efficiently for this purpose, which are classified as comparing distinctive configurations, parameter sweep, and global optimisation algorithms, as reviewed by Götteman et al. (2020). Similar reviews have also been reported by Golbaz et al. (2022), Teixeira-Duarte et al. (2022), and Yang et al. (2022). However, the topic in this paper is more focused on detailed design, which means that layout patterns are restricted to a small selection based on previous experience.

CONTACT Jonas W. Ringsberg  Jonas.Ringsberg@chalmers.se  Department of Mechanics and Maritime Sciences, Division of Marine Technology, Chalmers University of Technology, Gothenburg SE-412 96, Sweden

© 2024 The Author(s). Published by Informa UK Limited, trading as Taylor & Francis Group

This is an Open Access article distributed under the terms of the Creative Commons Attribution License (<http://creativecommons.org/licenses/by/4.0/>), which permits unrestricted use, distribution, and reproduction in any medium, provided the original work is properly cited. The terms on which this article has been published allow the posting of the Accepted Manuscript in a repository by the author(s) or with their consent.

Furthermore, this study provides detailed analyses of power performance.

Numerical tools are often utilised for the simulation and assessment of hydrodynamic and structural responses for WECs and the connected moorings and cables under the environmental loads of waves, winds, ocean currents, and sea ice. Numerical models based on different methods have been developed at different levels of complexity, for example, models using the boundary element method (BEM) (Lawson et al. 2014; Magkouris et al. 2020; Raghavan et al. 2022) and models using computational fluid dynamics (CFD) (Devolder et al. 2018; Li et al. 2022; Katsidoniotaki et al. 2023). A complete numerical analysis procedure based on the BEM for WEC systems has been established by the research group of the authors. Previous work has focused on a floating point absorber WEC developed by the Swedish company, Waves4Power. This single-unit WEC system is called WaveEL 3.0, and it has been evaluated and validated in a number of studies with regard to hydrodynamic performance, fatigue of mooring lines, mechanical life of the umbilical cable connected to the WEC, LCoE, life-cycle analysis (LCA), risk analysis, and the influence of biofouling on all of the system's components on energy production (Yang et al. 2018; Kuznecovs et al. 2019; Ringsberg et al. 2020a; Yang et al. 2020b). WaveEL 3.0 was also included in a recent study regarding the design of smaller wave farms (Yang et al. 2020a).

Notably, Waves4Power has developed a new generation of the WEC, which is termed WaveEL 4.0. WaveEL 4.0 is based on the design of WaveEL 3.0, but with a longer water tube and a slightly larger buoy diameter. WaveEL 4.0 is supposed to be installed in WEC arrays, and therefore, it is meaningful to compare the array performance of the two designs. Despite the experiences from previous studies on WaveEL 3.0, the complex hydrodynamic-mechanical coupling for this type of WEC technology requires a separate analysis to be performed for WaveEL 4.0. Since the mooring systems between the two generations are similar, the present study demonstrates how the WEC buoy dimensions affect hydrodynamic interaction effects for the same array layouts. Since the simulation methodology and model of WaveEL 3.0 have been validated in previous studies, the WaveEL 4.0 model can be assumed to be reliable for use in numerical simulations. Furthermore, Ringsberg et al. (2020a) assessed many array layouts and proposed candidate layouts for floating heaving point absorbers. Environmental conditions, incident wave directions, and the distances between WEC units were shown to have large impacts on moorings' fatigue life and the total power performance of an entire wave farm. In the current study, a new array layout design for 6 units distributed in a hexagonal pattern is introduced, which is developed by considering insights from previous studies and inspired by efficient biological structures in nature.

Hence, this study aims to provide a detailed analysis and comparison of the two WECs regarding their power performance and LCoE when installed in arrays. By comparing these two WEC configurations under the same installation and environmental conditions, the influence of hydrodynamic interactions can be estimated and used as guidance for future developments and full-scale unit deployment. LCoE calculations are performed to evaluate the layouts and clarify the extent to which the LCoE may be affected by hydrodynamic interaction effects.

The paper is arranged as follows. The numerical methods and simulation models are presented in Section 2. Parametric studies and the results are presented in Section 3. A discussion is presented in Section 4 before the study's conclusions are summarised in Section 5.

2. Methodology

A brief overview of the numerical methodology used in the study is presented in Sections 2.1–2.3, followed by a presentation of the simulation models in Section 2.4. The detailed description of the numerical methods and models have been described in former publications by the authors, in addition to validation studies carried out in ocean basin experiments and a verification study carried out on a full-scale installation of a single-unit WEC; see Yang (2018), Yang et al. (2020a) and Yang et al. (2020b). In these reports, extensive numerical studies and simulations were presented, demonstrating how the DNV Sesam software package should be used in both frequency-domain and fully coupled time-domain simulations, to capture hydrodynamic interaction effects between WECs installed in wave farms.

2.1. Hydrodynamic and structural response

Sesam is a software suite containing many useful tools and programmes for hydrodynamic and structural analyses of ships and offshore structures (DNV 2023). The tools and programmes used in this study are shown in Figure 1.

GeniE (GeniE 2023) is used to model the wet surface geometry of the floating body and divides the surface into multiple panels, which are inputs for calculating the hydrodynamic characteristics using the BEM. The Wadam programme (Wadam 2023) in HydroD (HydroD 2023) is used for hydrodynamic analysis in the frequency domain. It adopts the panel model created in GeniE to obtain the hydrodynamic characteristics, such as added mass, added damping, and wave excitation force transfer function, by solving the 3D linear velocity potential using the BEM. Note that the hydrodynamic interaction effects, namely the radiation and diffraction, are covered by the coupled added mass and damping, and wave excitation force transfer function, respectively.

The time-domain response is calculated using Sima (Sima 2023), which combines the two programmes, Simo (Simo 2023) and Riflex (Riflex 2023). Simo solves the equation of motions for the simulated body to get the motion responses in the time domain. It combines the load from the hydrodynamic analysis previously carried out in Wadam with the time-varying loads, such as the external forces from the power take-off (PTO) system and moorings. Riflex solves the mooring forces based on the motions of the simulated body at each time step during the simulation using the finite element method (FEM). Then, the instant mooring forces are input to Simo for a fully coupled simulation, which means that the mooring forces and motions of the body have a mutual and simultaneous influence. More detailed information on the theory behind the software has been described by Shao (2023).

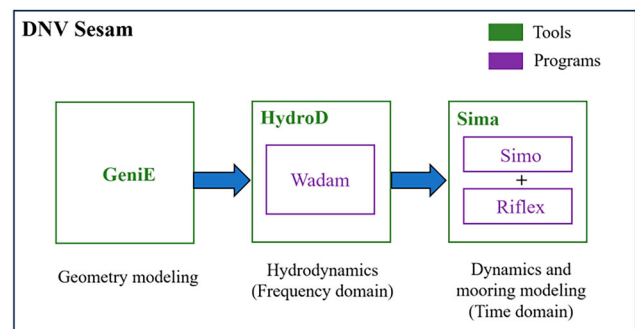


Figure 1. Tools and programmes of DNV Sesam used in this study.

2.2. Power performance analysis

Hydrodynamic interaction effects between WEC units in a wave farm can affect the motion characteristics of the units, and hence their power performance. In this study, although the WEC was modelled as a 6-degree-of-freedom (6-DOF) body in the time domain, only the motion in the heave direction was used to estimate the power performance. Furthermore, the PTO system was simplified as a linear damper that only acts in the heave direction. The total hydrodynamic power generation was calculated according to Equation (1), where B_{PTO} is the value of the linear damper, $\dot{\xi}$ is the time derivative of the heave motion, and T_{sim} is the simulation time. B_{PTO} was set to the value of the radiation damping at the resonance of the heave without the mooring system. For WaveEL 3.0, B_{PTO} is 40 kN/m, but for WaveEL 4.0, B_{PTO} is 50 kN/m. It should be noted that despite the simplicity of the modelling method, the model for WaveEL 3.0 has been verified against the measurements of this WEC in Runde, Norway; see Ringsberg et al. (2020b).

$$P = \frac{1}{T_{sim}} \int_0^{T_{sim}} B_{PTO} [\dot{\xi}(t)]^2 dt \quad (1)$$

2.3. LCoE analysis

This study followed the LCoE analysis procedure presented by Ringsberg et al. (2020a), Yang (2018), and Yang et al. (2020a). It is based on a cost definition model proposed by Castro-Santos et al. (2016a) and Castro-Santos et al. (2016b), who proposed that the LCoE (EUR/kWh) of a wave farm consisting of multiple units can be calculated as:

$$LCoE = \frac{\sum_{n=0}^{n=N} \frac{Cost_n}{(1+r)^n}}{\sum_{n=0}^{n=N} \frac{E}{(1+r)^n}} \quad (\text{unit: EUR/kWh}) \quad (2)$$

Where N is the target design operational life of the farm (in years), $Cost_n$ is the total cost (in EUR) of the wave farm in the n -th period (from year 1 to year N), E is the total annual energy production (in kWh) from all the WEC units, and r is the discount rate of the energy system (defined according to Costello and Pecher (2017)).

In this study, N was set to 25 years, and r was set to 0.09 according to Pecher and Kofoed (2017). The total annual energy production E of a wave farm depends on the number of WECs and the power performance of each WEC, calculated as:

$$E = \sum_{k=1}^{k=j} \bar{P}_k \cdot 24 \cdot 365 \cdot \eta_{Availability} \cdot \eta_{Transmission} \quad (3)$$

Where j denotes the total number of WEC units in the farm, the index k represents the k -th WEC in the wave farm, \bar{P}_k is the installed power performance of the k -th WEC in the farm at a particular operational site, $\eta_{Availability}$ is the fraction of time that a

particular operational site is available, and $\eta_{Transmission}$ is the transmission efficiency of the energy generated by each WEC to the final electricity output for the end user. The values of $\eta_{Availability}$, $\eta_{Transmission}$, and \bar{P}_k were taken from Yang et al. (2020a) and set to 0.95, 0.2, and 125 kW (for the WaveEL WEC), respectively. Irrespective of the WEC model and configuration of the WECs, the same value of \bar{P}_k was always used in Equation (3).

The life-cycle cost (LCC) calculation of the WEC farms followed the procedure proposed by Castro-Santos et al. (2016a, 2016b), which considers various cost aspects, including the cost of concept definition (C1), design and development (C2), manufacturing (C3), installation (C4), exploitation (C5), and dismantling (C6). This study followed the same assumptions as those described by Yang et al. (2020a), where all cost items, except costs related to the system and farm design, were estimated depending on the configuration and quantity of components employed in each WEC farm. The design costs were assumed to be identical for all WEC farms based on the fact that the design and selection process of various WEC farms had been performed as one integrated step; readers are referred to Ringsberg et al. (2020a). The design-related costs cover all of cost C2 and part of cost C1; cost C1 includes the cost of land usage, which was adjusted according to each WEC system. Table 1 summarises the LCoE estimation for an isolated WaveEL 4.0 unit and the four farms designed with different array layouts. Ringsberg et al. (2020a) have previously described the unit cost of various components in the system and Yang (2018) provided a complete list of assumptions for the LCoE calculations.

2.4. Simulation models

2.4.1. Single WEC unit

The main difference between WaveEL 3.0 and 4.0, as shown in Figure 2(a), is the length of the tube. WaveEL 4.0 has a longer tube, resulting in a lower centre of gravity (COG) and larger weight than WaveEL 3.0. The geometric parameters of the two WECs are presented in Table 2. These differences cause changes in the time-domain motion responses and power performance, which is calculated using Equation (1) based on the heave motion. However, it needs to be emphasised that the WECs were simulated as 6-DOF bodies in the time domain.

Figure 2(b) shows a single WaveEL 4.0 unit with its mooring system. WaveEL 3.0 is not shown here because the two units have the same mooring system. Three mooring lines spread out at an angle of 120°, and each mooring line contains two sections. The horizontal motion is constrained by the horizontal section, which is denoted as section 1. The vertical section is denoted as section 2 and is connected to the anchor at the seabed. To prevent snap loads, three floaters are applied to each leg to keep the moorings in tension. Sections 1 and 2 are connected by a floater. According to Waves4Power's design, the pre-tension at each mooring leg in static water conditions is 47 kN. More details about the WEC system and mooring line properties have been previously outlined by Yang et al. (2020a).

Table 1. LCoE costs of an isolated WaveEL 4.0 unit and the four farms with different array layouts. The definition of different layouts can be found in Section 2.4.2; Ringsberg et al. (2020a) provided a detailed presentation of all the financial parameters and costs.

Costs [EUR]	Isolated unit	Hex1-80	Hex1-120	Hex2	StarBuoy
Concept definition, C_1	3,164,467	3,172,738	3,469,703	4,819,595	3,429,219
Design and development, C_2	2327	2327	2327	2327	2327
Manufacturing, C_3	867,908	4,097,553	4,104,187	4,147,660	6,693,678
Installation, C_4	116,896	413,160	413,160	666,160	691,600
Exploitation, C_5	1,975,377	4,920,796	5,637,277	6,185,174	11,424,737
Dismantling, C_6	20,874	60,390	60,390	60,390	91,990
Sum of costs C_1 - C_6 , LCC	6,147,848	12,666,937	13,687,017	15,881,280	22,333,525

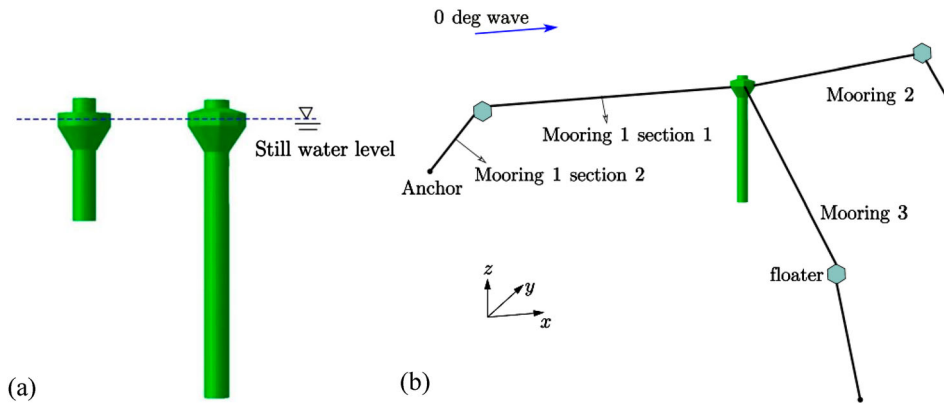


Figure 2. (a) The geometries of WaveEL 3.0 (left) and WaveEL 4.0 (right); (b) an isolated WaveEL 4.0 unit with moorings (Shao et al., 2023).

2.4.2. Array layouts

Ringsberg et al. (2020a) used systems engineering to propose 22 conceptual mooring solutions for different array layouts of WaveEL 3.0. They were systematically compared and reduced to four top concepts using the Pugh and Kesselring matrices. The top concepts were assessed in detail by considering the LCoE, LCA, and risk analyses. The fatigue life of the mooring lines and the energy capture were calculated using results obtained from coupled hydrodynamic and structural response analyses. The StarBuoy concept – an array layout with 10 units – was found to be the most effective alternative for the conditions simulated outside Runde in Norway.

The StarBuoy layout was investigated in the current study together with two new layouts, Hex1 and Hex2, which are 6-unit hexagonal arrays. They evolved from the StarBuoy layout to be optimised for alternating incident wave directions and environmental conditions. Their shapes are shown in Figure 3(a), and their key parameters are listed in Table 3 where R is the radius of the total footprint area of each array, r is the radius of a single unit, and the distance between units is defined as the distance between two adjacent units. The key parameters of the array layouts were determined using the procedure described by Ringsberg et al. (2020b). The motivation for the Hex1 and Hex2 designs is that smaller wave farms with fewer units have additional advantages that can help reduce the LCoE based on rated power (i.e. interaction effects were disregarded), LCC, and mitigate risks, according to Ringsberg et al. (2020a).

The three layouts are interconnected with similar parameters. An evolution roadmap is shown in Figure 3(b). Hex1-120 was obtained by having a similar R as StarBuoy to keep a similar footprint area. To decrease the total mooring length, a shorter distance between units, 80 m, was applied and that new layout was called Hex1-80. Hex2 and Hex1-120 share similar single unit radius r . The difference between them is that Hex1-120 is more compact and shares a centre anchor, whereas Hex2 does not share a centre anchor and consequently has a larger array radius R . This changed arrangement of anchors for mooring lines is expected to affect LCoE, maintenance, and the LCA.

Table 2. Geometric parameters of the two WEC configurations.

Parameter	WaveEL 3.0	WaveEL 4.0
COG [m] (the origin is at the still water level)	-1.9	-10.6
Weight [kg]	140,000	217,000
Tube length [m]	10.7	37.1
Buoy diameter [m]	8	8.6
Tube outer diameter [m]	3.5	3.5

2.4.3. Environmental conditions

The numerical simulations were limited to regular waves and four incident wave directions ranging from 150° to 180° , as depicted in Figure 3(a). The WEC arrays were studied under three representative environmental conditions (i.e. EC1–3) selected based on the representative wave scatter diagram of the Runde (Norway) test site of Waves4Power’s WaveEL 3.0 (Ringsberg et al. 2020b). EC1 and EC2 represent the two most frequently observed sea states during the period from June to November 2017 in Runde (Norway), and EC3 is a sea state with a relatively larger wave amplitude and period and a lower probability of occurrence, see Table 4. These conditions belong to the linear and weakly nonlinear wave theory regions. The variation in incident wave directions was also typical for the conditions observed during the experimental campaign in 2017. Notably, since the effects of wind and current are not considered in this study, each environmental condition is simply a sea state condition. Hereafter, the term environmental condition is used for consistency with previous studies of the authors (see, e.g. Yang et al. (2020a)).

3. Results

3.1. Performance of single WEC unit

The heave response amplitude and power absorbed by a single WEC unit are shown in Figure 4. WaveEL 4.0 generally outperforms WaveEL 3.0, although the incremental power gained using WaveEL 4.0 is nearly negligible under EC1 with small regular waves. In the moderate condition, EC2, WaveEL 4.0 absorbs twice the power (28 kW) of WaveEL 3.0. A noticeable improvement is also observed for EC3 with extremely large regular waves, where WaveEL 4.0 absorbs 55% more power than WaveEL 3.0.

The significantly improved power absorption from WaveEL 4.0 was also reported in a recent study (Shao et al. 2023), where these two WEC concepts were simulated over a wide set of wave conditions, $A \in [0.25, 3]$ m and $T \in [4.5, 7.5]$ s. The motion trajectories predicted using the present simulation method vary in the ranges that agree with full-scale on-site measurements. The numerical and experimental results also show similar axial mooring forces.

According to Equation (1), the power absorption is positively correlated to the amplitudes of buoy heaving motions and the damper coefficient B_{PTO} . Since B_{PTO} is constant (40 kN/m for WaveEL 3.0 and 50 kN/m for WaveEL 4.0), the change in this parameter accounts for a 25% increase in power generation. However, the power increase owing to the upgrades of WaveEL 4.0 is much smaller than 20% for EC1 and beyond 55% for EC2 and EC3. The reason

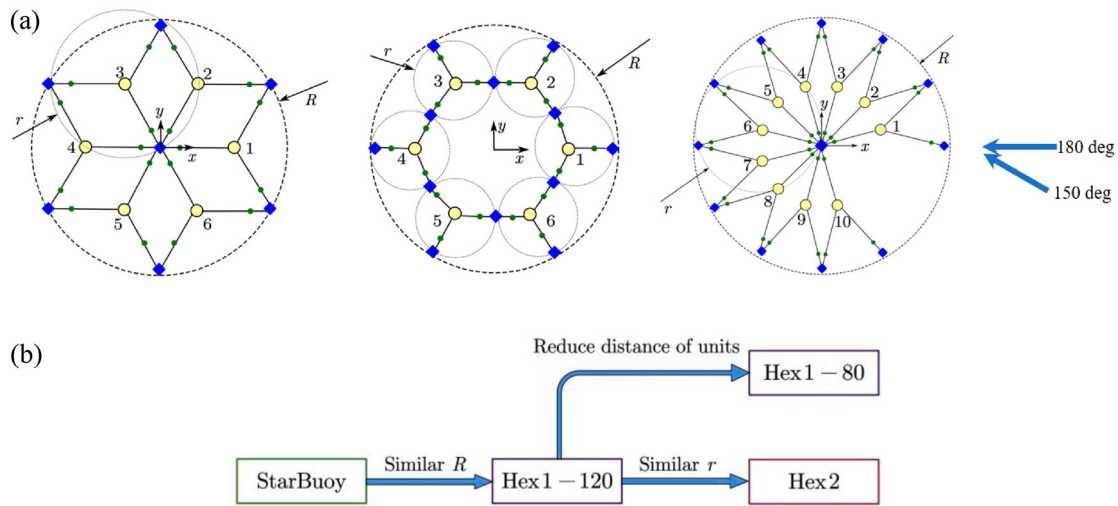


Figure 3. (a) Three array layouts for WEC farms. The numbered yellow circles show the WEC units, green circles show the floaters, and blue squares show the anchors. From left to right: Hex1 (with a distance of 80 or 120 m for Hex1-80 or Hex1-120, respectively), Hex2, and StarBuoy. Examples of incident wave directions are marked with blue arrows. (b) The evolution roadmap of the three studied array layouts.

Table 3. Key parameters of the conceptual array layouts.

Layout	Number of units	Distance of units [m]	R [m]	r [m]
Hex1-80; Hex1-120	6, sharing a centre anchor	80; 120	139; 208	80; 120
Hex2	6, not sharing a centre anchor	260	390	130
StarBuoy	10 (Yang et al. 2020a)	52	200	100

is that the design of WaveEL 4.0 is more effective at generating time-varying heaving motions in response to incoming waves. The most critical difference between the two WEC concepts is the water tube length. In addition, the difference in the axial mooring forces is less than 5% according to a previous study (Shao et al. 2023). The improved power generation from the new design of WaveEL 4.0 is mainly related to the length extension of the water tube underneath the buoy, leading to more effective resonance and larger radiation damping in the given environmental conditions. This is confirmed in Figure 4(b) where the heave amplitude response is higher for WaveEL 4.0 with a wave period larger than 4.5 s. A more detailed study of the physical mechanisms correlating the design parameters (geometrical and mechanical) and power generation should be explored in future work.

3.2. Effects of environmental conditions

The normalised power absorbed by the units in the Hex1-80 layout with an interval WEC distance of 80 m, which has a shared central anchor, subject to the incoming wave angle of 180°, is displayed in Figure 5. It is worth noting that the polar coordinate system is used to show the unit locations and normalised hydrodynamic power.

Table 4. Definition of three environmental conditions selected for detailed study by numerical simulations.

EC	Wave amplitude, A [m]	Wave period, T [s]	Wavelength [m]	Occurrence probability [%]
EC1	0.25	4.5	31.6	6.84
EC2	0.75	5.5	47.2	10.14
EC3	1.75	7.5	87.8	5.63

The distance between each point in Figure 5 and the origin stands for the normalised hydrodynamic power. The WEC locations and numbers are shown in Figure 3(a). The hydrodynamic power of the array units for a given environmental condition is normalised based on the corresponding power of the single units for the same condition, which is indicated in Figure 4(b). Similarly, the hydrodynamic power of the single unit is normalised to be $\bar{P}_{ref} = 1$. Therefore, a physical interpretation of the normalisation strategy is that, once a normalised value is not equal to one (i.e. \bar{P}_{ref}), the hydrodynamic interactions between the WEC units affect the energy harvesting performance. Hereafter, this normalisation strategy is applied to the analysis of the power absorption in relation to the interaction effects.

The performances of most of the WEC units are enhanced for EC1 and EC2 because of the constructive interactions, except for the upstream units at 60° and 300° for WaveEL 4.0, as shown in Figure 5(a,b). The most efficient unit in all cases is located at 180°, which is the most upstream position. Moreover, the array of WaveEL 4.0 units is more sensitive to environmental conditions and exhibits higher performance in EC1 and EC2 compared with EC3. The sensitivity is mainly attributed to the length extension of the water tube and the resulting change in radiation damping. Figure 5(c) shows the power performance of WaveEL 4.0 but normalised by the reference values of WaveEL 3.0. Each WaveEL 4.0 unit in the array absorbs at least 1.5 times more power than that of the corresponding WaveEL 3.0 unit under the same environmental conditions.

In contrast to EC1 and EC2, the power polar maps of both WEC concepts for EC3 almost overlap with that of \bar{P}_{ref} . This implies that the interaction effects are negligible in extreme environmental conditions with large waves. Since the wavelength of EC3 is significantly larger than the WEC buoy diameter, which is 8 m for WaveEL 3.0 and 8.6 m for WaveEL 4.0, the buoys cannot deflect or reflect the waves.

The total power absorbed by the arrays is normalised by six times the power of the single unit (see Figure 4(b)), considering that the hexagon layout contains six units. The normalisation results, \bar{P}_{tot} , of Hex1-80 with an incident wave angle of 180° are shown in Figure 6. For EC1 and EC2, an array of units working constructively is much more efficient than a set of individual units working independently. Especially for EC2, the Hex1-80 layout

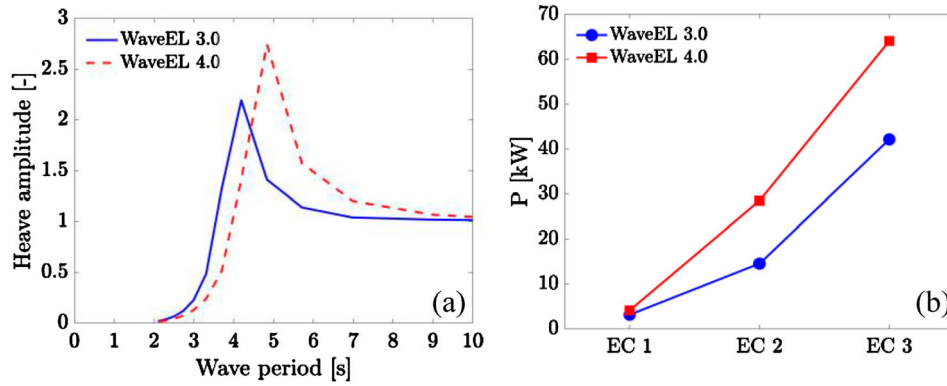


Figure 4. (a) Heave amplitude response per unit wave height with respect to wave period (Shao et al., 2023). (b) power generation of the isolated single WEC units under different environmental conditions (EC1 to 3).

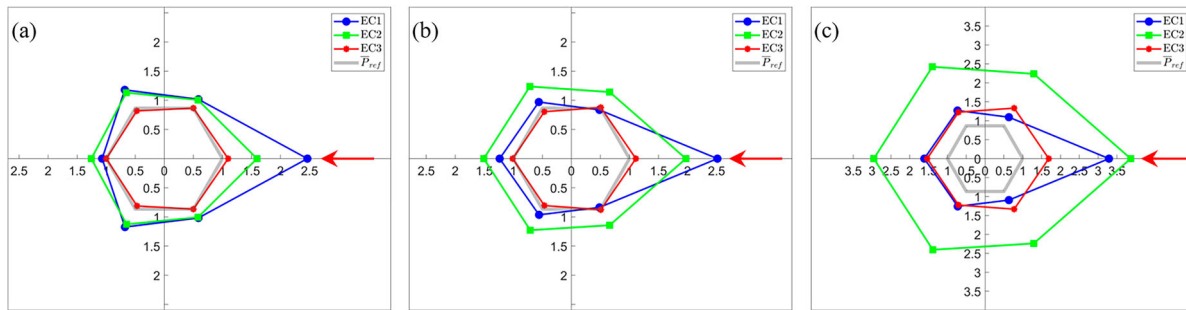


Figure 5. Normalised power absorbed by each WEC unit in the Hex1-80 layout for (a) WaveEL 3.0, (b) WaveEL 4.0, and (c) WaveEL 4.0 but normalised with the reference value of WaveEL 3.0. The incoming wave angle is 180° , which is marked with red arrows. The polar coordinate system is used here, and the unit positions are indicated in Figure 3(a).

can increase the power absorption by 30% (derived from 1.3 in the figure) for WaveEL 3.0 and 50% for WaveEL 4.0.

For EC3 with large waves, the normalised total power of the arrays for both WEC models is approximately equal to one. Therefore, Hex1-80 has neither a constructive nor a destructive effect on hydrodynamic energy harvesting. This behaviour is understandable in terms of the unit performances indicated in Figure 5.

Only three representative regular wave conditions were examined in this study to distinguish the basic characteristics of the WEC models and layouts. However, real environmental conditions are more complex, and waves are generally short-crested and

irregular. Nonetheless, the simplifications introduced in this study are necessary to reduce the complexity. Similarly, the PTO system is modelled as a linear damper, which is only reasonable under selected environmental conditions. More complex PTO system modelling is necessary for short-crested and irregular waves and long-term annual power assessment.

3.3. Effects of incoming wave directions

Given the symmetric topology of the hexagon shape, the whole array performance is dependent on the incident wave direction ranging from 150° to 180° . The array layout with the interval unit distance of 80 m, Hex1-80, for EC2 with moderate waves is shown for four incident wave directions in Figure 7. A similar trend with respect to the incident wave direction is observed for WaveEL 3.0 and 4.0. The unit farthest upstream harvests the most power at 180° , whereas the two units most downstream have the most power at 150° . The interaction effects are constructive for all wave directions, although they are minor for the upstream units with an incident wave angle of 150° .

Moreover, the performance of WaveEL 4.0 is strengthened more by the Hex1-80 layout, compared with WaveEL 3.0. However, as shown in Figure 7(b), the upstream WaveEL 4.0 units are more strongly affected by the incident wave direction. For brevity, the wave-direction effects for EC1 and 3 are not shown here. It was found that the array units behave similarly in EC1 and 2, whereas the units operate like single units with no interactions in EC3. As mentioned above, the wavelength of EC3 is much larger than the

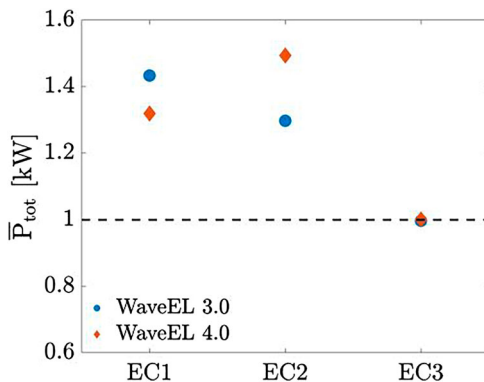


Figure 6. Normalised total power of the Hex1-80 layout with the incident wave direction of 180° .

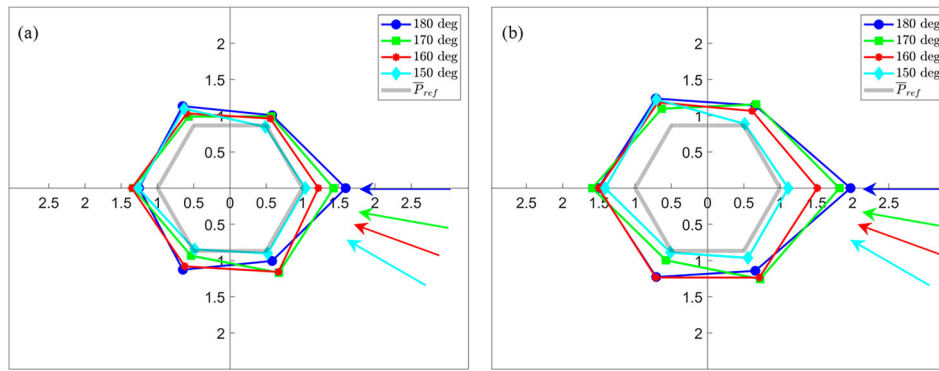


Figure 7. Normalised power output from each WEC unit in the Hex1-80 layout under EC2, using (a) WaveEL 3.0 and (b) WaveEL 4.0. The arrows indicate the incident wave directions.

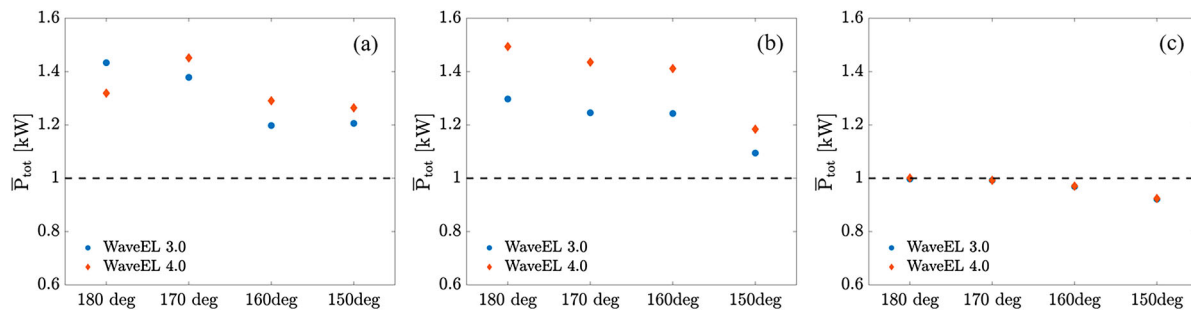


Figure 8. Normalised total power of the Hex1-80 layout with different incident wave directions under the various environmental conditions: (a) EC1, (b) EC2, and (c) EC3.

WEC buoy diameter, resulting in negligible interactions between the waves and the buoys.

The normalised total power of the Hex1-80 layout subject to the different incident wave directions is displayed in Figure 8. For EC1 and EC2, the layout yields a larger power increase for WaveEL 4.0 than for WaveEL 3.0. The only exception is EC1 for a wave direction of 180°, where WaveEL 3.0 outperforms WaveEL 4.0 by 10%. At incident wave directions of 150° and 160° for EC1, the power increases are less than those for the other two angles. These results for small waves in EC1 are different from those observed for moderate waves in EC2. The power increase in EC2 is minimal when the incident wave direction is 150°, and it is approximately 5% for WaveEL 3.0 and 10% for WaveEL 4.0. Although the power increase drops at 150° in EC2, it remains at 25–30% for WaveEL 3.0 and 40–50% for WaveEL 4.0. Therefore, the layout introduces more constructive interaction effects to absorb the hydrodynamic power from low and moderate waves, especially for WaveEL 4.0.

As shown in Figure 8(c), for EC3 with large waves, the normalised power of the arrays is close to one for the wave directions of 170° and 180°, indicating that the interaction effects are negligible. Moreover, the interactions result in normalised power absorptions of less than one at 150° and 160°. This means the interactions degrade the energy harvesting performance. The situation is worse at 150° than at 160°. Therefore, Hex1-80 is ineffective and potentially harmful to the WEC performance depending on the conditions, given that the wavelengths (e.g. 87.8 m in EC3) can be much larger than the buoy diameters (8 m for WaveEL 3.0 and 8.6 m for WaveEL 4.0) and that the wave frequencies are much smaller than the WEC resonant frequencies (1.6 rad/s for WaveEL 3.0 and 1.3 rad/s for WaveEL 4.0).

3.4. Comparison of 6-WEC array layouts

The Hex1-120 and Hex2 layouts are compared in Figure 9 and Figure 10. Only EC2 and EC3 are considered since the units are most efficient in EC2 and EC3. The Hex1-80 layout is ineffective as shown in Figure 8(c). The Hex1-120 layout is chosen instead of Hex1-80 because the length of its mooring lines and the radius of a single WEC unit are more comparable to those of Hex2 (see Table 3 and Figure 3(a)). In other words, the geometric parameters are more similar. The incident wave directions of 150° and 180°, which are aligned with the symmetry axes of the hexagon, are also shown in Figure 9 and Figure 10.

For WaveEL 3.0, Hex2 slightly outperforms Hex1-120 under EC2 for the two incident wave directions. The performance of WaveEL 3.0 is relatively stable for various layouts and incident wave directions, and the interaction effects are consistently produced. In contrast, for WaveEL 4.0, Hex2 is outperformed by Hex1-120 under EC2. The differences in the normalised power between the two array layouts are large, and the hydrodynamic power in Hex1-120 is more evenly distributed among the units. These observations indicate that the interaction effects of WaveEL 4.0 are more dependent on the layout topology, and the most stability is achieved using Hex1-120. Considering that the critical difference between WaveEL 3.0 and 4.0 is the water tube length, the length extension is likely the reason why WaveEL 4.0 is more sensitive to the interaction effects, and consequently, more dependent on the layout topology. Furthermore, the performance is always improved compared with the individual units, regardless of the layout.

Under EC3, as shown in Figure 10, the performance of each WEC shows almost the same or slightly smaller power generation than the reference value, regardless of the layout and incoming

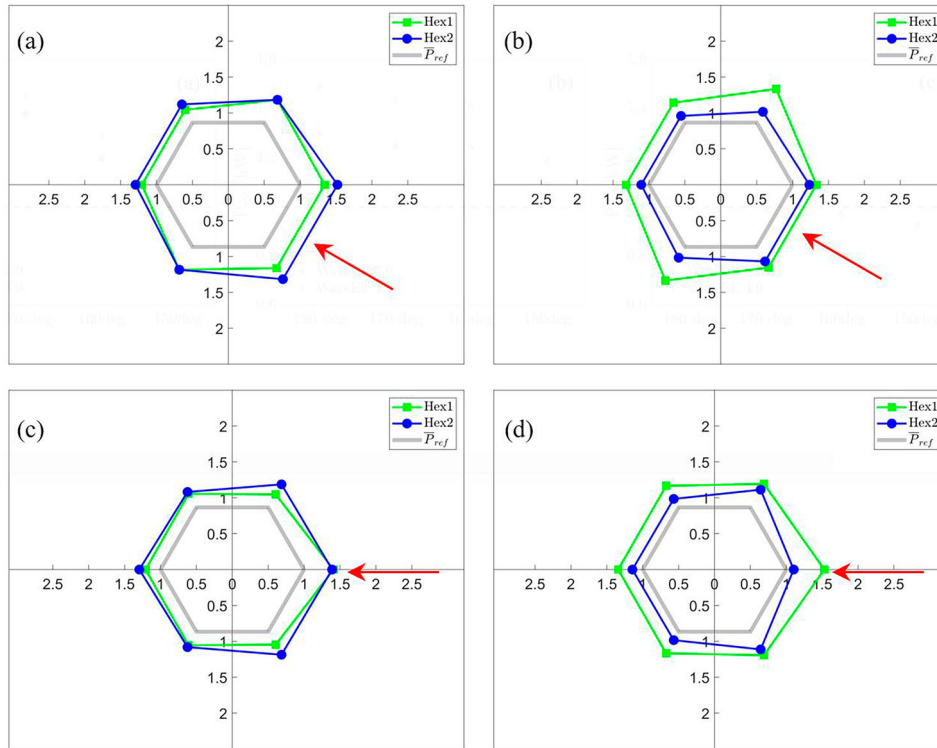


Figure 9. Normalised power generated from each WEC unit in the Hex1-120 and Hex2 layouts under EC2 with the incident wave direction of 150° for (a) WaveEL 3.0 and (b) WaveEL 4.0, and 180° for (c) WaveEL 3.0 and (d) WaveEL 4.0. Note that the polar coordinate system is used here, and the unit positions correspond to Figure 3(a). The red arrows indicate the incident wave directions.

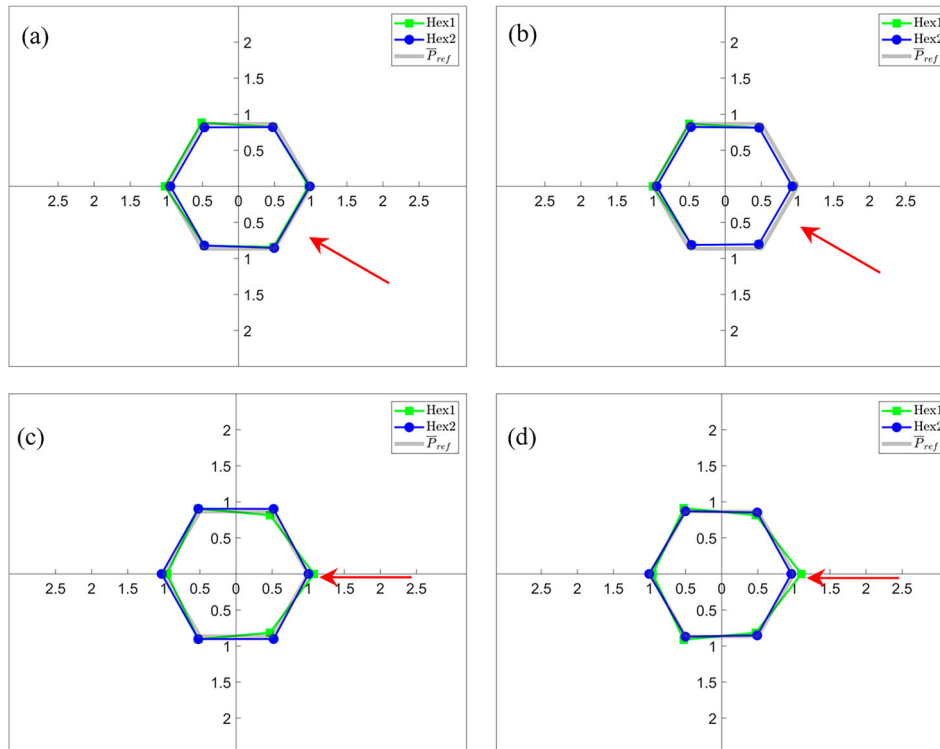


Figure 10. Normalised power generated from each WEC unit in the Hex1-120 and Hex2 layouts under EC3 with the incident wave direction of 150° for (a) WaveEL 3.0 and (b) WaveEL 4.0, and 180° for (c) WaveEL 3.0 and (d) WaveEL 4.0. Note that the polar coordinate system is used here, and the unit positions correspond to Figure 3(a). The red arrows indicate the incident wave directions.

wave angle. This is consistent with the results observed in Figure 8 (c) for the Hex1-80 layout.

3.5. The influence of interaction effects on LCoE

The hydrodynamic interaction between WECs in a wave farm affects the value of the LCoE (i.e. $LCoE_{interact} = (LCoE_{no\ interact})/I_p$). Here, I_p is the interaction factor of the hydrodynamic power, and it is defined as $I_p = P_{interact}/P$, for the estimated power performance considering interaction effects normalised by the estimated power performance when the interaction effects are not considered in the simulation model (Yang et al. 2020a). A value of I_p larger than unity means more power is produced because of the hydrodynamic interaction effects. Hence, an I_p larger than unity reduces the estimated value of the LCoE, and a value less than unity increases the value of the LCoE. Table 5 and Table 6 present simulation results of the power interaction factors I_p that have been calculated for the studied wave farms. Notably, the incident wave directions and EC1–3 result in different interaction factors; hence, the scatter diagram should be used for more precise estimation at an installation site. Table 7 presents the average values of I_p . These values were used to calculate the LCoE values, adjusted based on hydrodynamic interaction effects, see Table 8.

The results in Table 8 show that hydrodynamic interaction effects can significantly reduce the LCoE value. The StarBuoy layout with WaveEL 4.0 has the lowest LCoE value and the Hex1-120 layout with WaveEL 4.0 has the second lowest LCoE value. The Hex2 layout has the largest LCoE among the studied wave farms. Based on the simulated conditions of EC1 to EC3, WaveEL 4.0 appears to be more energy- and cost-efficient than WaveEL 3.0.

4. Discussion

4.1. Interaction effects for the studied arrays and WEC systems

The normalised total power of the entire arrays in the three conditions, EC1–3, is shown in Figure 11. In EC1, the Hex2 layout with WaveEL 3.0 has the highest performance for all incident

Table 5. Power interaction factors I_p [-] for Hex1-80, Hex1-120, and Hex2.

WaveEL; EC	Incident wave direction [deg.]	Hex1-80	Hex1-120	Hex2
3.0; EC1	150	1.21	1.44	1.86
	160	1.20	1.19	1.80
	170	1.38	1.25	1.80
	180	1.43	1.05	1.80
3.0; EC2	150	1.09	1.30	1.40
	160	1.24	1.15	1.32
	170	1.25	1.07	1.34
	180	1.30	1.25	1.35
3.0; EC3	150	0.92	0.98	0.96
	160	0.97	0.98	0.98
	170	0.99	0.99	1.03
	180	1.00	1.00	1.03
4.0; EC1	150	1.26	1.76	1.10
	160	1.29	1.48	1.02
	170	1.45	1.44	1.02
	180	1.32	1.22	1.09
4.0; EC2	150	1.18	1.44	1.17
	160	1.41	1.31	1.14
	170	1.44	1.18	1.16
	180	1.49	1.39	1.22
4.0; EC3	150	0.92	1.44	0.94
	160	0.97	1.31	0.97
	170	0.99	1.18	0.99
	180	1.00	1.01	0.99

Table 6. Power interaction factors I_p [-] for StarBuoy with WaveEL 4.0 under EC2.

Wave encounter direction [deg.]	I_p [-]
150	1.41
165	1.45
180	1.63
195	1.59
210	1.67
225	1.66
240	1.70
255	1.68
270	1.81
285	1.68
300	1.51
315	1.57
330	1.39

Table 7. Mean values of the interaction factors I_p [-] in Table 5 and Table 6.

WaveEL; EC	Hex1-80	Hex1-120	Hex2	StarBuoy
3.0; EC1	1.31	1.23	1.82	N.A.
3.0; EC2	1.22	1.19	1.35	N.A.
3.0; EC3	0.97	0.99	1.00	N.A.
4.0; EC1	1.33	1.48	1.06	N.A.
4.0; EC2	1.38	1.33	1.17	1.60
4.0; EC3	0.97	1.24	0.97	N.A.

wave directions compared with the other configurations. Moreover, the total power remains nearly the same for the different wave directions. This even distribution is also found for this configuration in EC2 and EC3, although the performance improvement is dramatically reduced from 70% (derived from 1.7 in the figure) in EC1 to 20–50% in EC2 and approximately 0% in EC3. This means that the interaction effects from the Hex2 layout with WaveEL 3.0 are not sensitive to the incident wave direction or the environmental conditions.

In EC2, the Hex2 layout with WaveEL 3.0 is less efficient than Hex1-120 with WaveEL 4.0, where the power absorption of WaveEL 3.0 is two times smaller than that of WaveEL 4.0 (see Figure 4(b)). EC2 is an ideal environmental condition under which the present WECs exhibit the greatest performance enhancements from the interaction effects. Notably, the wavelength in EC2 is 5 times larger than the buoy diameter, and the wave frequency is comparable to the WEC characteristic frequency. Based on Figure 4 (b) and Figure 11, the most efficient configuration under EC2 is Hex1-120 with WaveEL 4.0. The only minor weakness is that the normalised power is reduced from 1.5–1.2 (i.e. by 30%) when the incident wave direction is changed from 180° to 150°.

In EC3, the interaction effects are very small or slightly detrimental to power absorption, as seen in Figure 11. This observation is consistent with the results of the preceding analyses. The individual WEC units are nearly decoupled from each other owing to the large length and frequency differences between them and the waves.

Table 8. LCoE [EUR/kWh] estimated with/without the power interaction factors I_p presented in Table 7.

	Hex1-80	Hex1-120	Hex2	StarBuoy
Assume $I_p = 1$	0.76	0.80	0.94	0.72
3.0; EC1	0.58	0.65	0.52	N.A.
3.0; EC2	0.62	0.67	0.70	N.A.
3.0; EC3	0.78	0.81	0.94	N.A.
Mean value: 3.0 EC1-EC3	0.66	0.71	0.72	N.A.
4.0; EC1	0.57	0.54	0.89	N.A.
4.0; EC2	0.55	0.60	0.80	0.45
4.0; EC3	0.78	0.65	0.97	N.A.
Mean value: 4.0 EC1-EC3	0.64	0.60	0.89	0.45

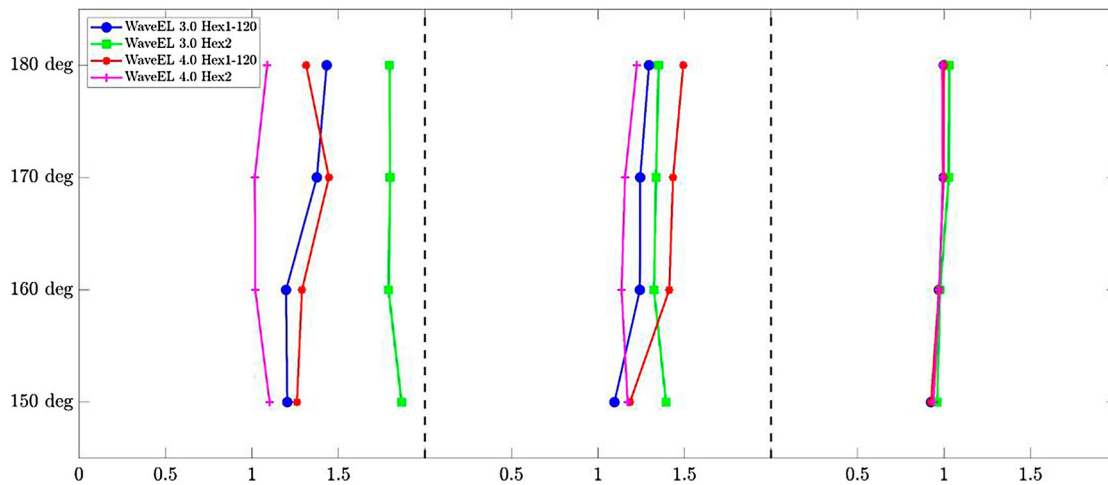


Figure 11. Normalised total power from the entire layouts, Hex1-120 and Hex2, using WaveEL 3.0 and 4.0 under the different environmental conditions, EC1–3.

Moreover, unlike Hex1 and Hex2, StarBuoy has only one symmetry axis (see Figure 3(a)). Thus, seven wave directions from 150° to 330° were simulated in Figure 12. Compared with Hex1 and Hex2, StarBuoy has a larger normalised total power and a minimum performance improvement of 40% (derived from 1.4 with the incident wave direction equal to 150° and 330° in Figure 12). However, one major disadvantage of StarBuoy is that the total performance is sensitive to the incident wave direction.

4.2. Array design and LCoE values

Section 2.4.2 presents the procedure to define the studied arrays and the motivation for their selections. The procedure was established and presented by Ringsberg et al. (2020a), and it is based on a systems engineering methodology where results from LCoE, LCA, and risk analyses together form the basis for decision-making of the most promising WEC array designs. The authors recommend adopting such a procedure since if too much emphasis is only on the hydrodynamic performance to minimise the LCoE, which is often the case in the public literature, the LCoE value will, in the end, likely be erroneous and too optimistic.

Research on optimising wave farms as large arrays or an intelligent combination of smaller clusters of arrays that form large-scale wave farms is evolving, see e.g. Giassi et al. (2020) and Götteman et al. (2020). All WEC systems have unique designs. Knowledge transfer between WEC systems belonging to the same category of PTO work principle (e.g. floating point absorber) is essential,

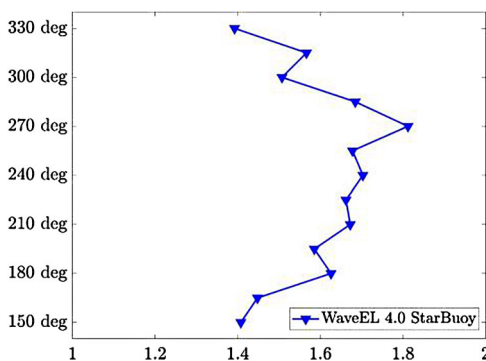


Figure 12. Normalised total power from the entire StarBuoy layout for incident wave directions of 150° to 330°, using StarBuoy with WaveEL 4.0 under EC2.

especially when installed in arrays. The design of arrays will be different between WEC systems and WEC PTO work principle. LCoE analysis is, therefore, one of the vital assessment tools needed to compare different WEC systems and their array designs. The authors recommend that LCA and risk analyses be included in the early design to discard less realistic array designs.

The influence of interaction effects on LCoE for the studied WEC system is presented in Section 3.5. For comparison, examples of LCoE values from other studies are presented in Table 9. Overall, the LCoE calculated in this study is slightly higher, likely because all possible costs have been included in this study. The examples from these studies confirm the findings in the current study that the value of the LCoE is strongly influenced by the unit WEC systems design, the distance between the WECs in an array, and the total number of WECs in the array.

5. Conclusions

This study investigated the power performance of two WaveEL WECs used in three different wave farm layouts under three environmental conditions, EC1 to EC3, with regular waves. The wave amplitude, wave period, and incident wave directions were varied for each environmental condition. Although the real environmental conditions in nature involve short-crested and irregular waves, using regular waves helps clarify the basic characteristics of the WEC models and layouts. The power performances of a single WEC unit and a WEC array are highly related to the

Table 9. LCoE from other studies for comparison.

References	Description	LCoE (EUR/kWh)
Sandberg et al. (2016)	1 WECs, CorPower WEC	0.633
	2 WECs, CorPower WEC	0.282
	4 WECs, CorPower WEC	0.310
Sergent et al. (2020)	Oscillating float, $r = 0.1$	0.27–0.37
	Oscillating float, $r = 0.075$	0.23–0.32
Giassi et al. (2020)	10 WECs, interaction cutoff distance 40 m or 100 m	0.240 (40 m); 0.245 (100 m)
	20 WECs, interaction cutoff distance 40 m or 100 m	0.238 (40 m); 0.242 (100 m)
	50 WECs, interaction cutoff distance 40 m or 100 m	0.245 (40 m); 0.247 (100 m)
Oliveira-Pinto et al. (2019)	Bref-SHB, point absorber	0.389
	F-HBA, point absorber	0.188
	Bref-HB, point absorber	0.428
	F-2HB, point absorber	0.220

environmental conditions. WaveEL 4.0 showed a 55% increase in power generation under EC3 compared with WaveEL 3.0. Owing to the interaction effects, the power performance of each WEC in array layout Hex1 either increased or slightly decreased, and the most efficient unit in all cases is the one located at the positive x -axis when the waves come from 180° . The highest normalised total power performance of Hex1-80 with WaveEL 3.0 occurred under EC1, but for the same layout but with WaveEL 4.0, the highest normalised power performance occurred under EC2. The normalised total power performance under EC3 was close to unity, which implies that there is no significant difference due to interaction effects. The incoming direction of the wave also plays an important role in power performance. Accordingly, the performance of the upstream units of WaveEL 4.0 was more sensitive to the change in the incident wave direction. Regarding the effects of the array layout on power performance, Hex2 with WaveEL 3.0 outperformed Hex1-120, whereas Hex2 with WaveEL 4.0 was outperformed by Hex1-120 under EC2 with waves coming from 150° and 180° . The individual performances of WEC units were practically decoupled from each other under EC3. StarBuoy generally showed a high power performance, but it was sensitive to the incoming wave angle. Overall, the three layouts all exhibited enhanced power generation compared with isolated units since the hydrodynamic interactions introduced constructive effects in most of the environmental and operating conditions.

The LCoE values indicate that the StarBuoy layout is the most economical. The layout with the second lowest LCoE was Hex1-120 with WaveEL 4.0. Furthermore, WaveEL 4.0 appears to be more energy- and cost-efficient than WaveEL 3.0 based on the simulated environmental conditions. The LCoE values calculated in this study were slightly higher than those obtained in similar studies because of the inclusion of all possible costs.

Disclosure statement

No potential conflict of interest was reported by the author(s).

Funding

This work was performed within the project entitled ‘Control of wave energy converters based on wave measurements, for optimal energy absorption,’ funded by the Swedish Energy Agency through contract agreement no. 50197-1, and ‘INTERACT – Analysis of array systems of wave energy converters with regard to interaction effects in the LCoE and fatigue analyses,’ funded by the Swedish Energy Agency through contract agreement no. 50148-1. This study also received funding from the Chalmers University of Technology Foundation for the strategic research project ‘Hydro- and aerodynamics’. Göran Fredriksson and Jonas Kamf from Waves4Power (<https://www.waves4power.com>) are acknowledged for their contributions to technical discussions and for sharing information on the WaveEL WECs.

Data availability statement

There is no data availability statement.

ORCID

Jonas W. Ringsberg  <http://orcid.org/0000-0001-6950-1864>

References

- Babarit A. 2010. Impact of long separating distances on the energy production of two interacting wave energy converters. *Ocean Eng.* 37(8-9):718–729. doi:10.1016/j.oceaneng.2010.02.002.
- Babarit A. 2013. On the park effect in arrays of oscillating wave energy converters. *Renew Energy.* 58:68–78. doi:10.1016/j.renene.2013.03.008.

- Borgarino B, Babarit A, Ferrant P. 2012. Impact of wave interactions effects on energy absorption in large arrays of wave energy converters. *Ocean Eng.* 41:79–88. doi:10.1016/j.oceaneng.2011.12.025.
- Budal K. 1977. Theory for absorption of wave power by a system of interacting bodies. *J Ship Res.* 21(4):248–254. doi:10.5957/jsr.1977.21.4.248.
- Castro-Santos L, Martins E, Soares CG. 2016a. Methodology to calculate the costs of a floating offshore renewable energy farm. *Energies.* 9(5):324. doi:10.3390/en9050324.
- Castro-Santos L, Martins E, Soares CG. 2016b. Cost assessment methodology for combined wind and wave floating offshore renewable energy systems. *Renew Energy.* 97:866–880. doi:10.1016/j.renene.2016.06.016.
- Child BFM, Venugopal V. 2010. Optimal configurations of wave energy device arrays. *Ocean Eng.* 37(16):1402–1417. doi:10.1016/j.oceaneng.2010.06.010.
- Costello R, Pecher A. 2017. Economics of WECs. *Handbook Ocean Wave Energ.* 101–137.
- Devolder B, Stratigaki V, Troch P, Rauwoens R. 2018. CFD simulations of floating point absorber wave energy converter arrays subjected to regular waves. *Energies.* 11(3):641. doi:10.3390/en11030641.
- DNV. 2023. Home page of DNV Sesam software. Available at: https://www.dnv.com/services/strength-assessment-of-offshore-structures-sesam-software-1068?utm_campaign=structure_sesam&utm_source=google&utm_medium=cpc&gad=1&gclid=Cj0KCQjw7uSkBhDGARIsAMCZNJvPMYbW5BYmxHGL8h1q54cjt_uNVB8_1-ufAkafk5_qYRCjYl7kIaAhQ3EALw_wcB&gclsrc=aw.ds.
- Engström J, Eriksson M, Götteman M, Isberg J, Leijon M. 2013. Performance of large arrays of point absorbing direct-driven wave energy converters. *J Appl Phys.* 114(20):204502. doi:10.1063/1.4833241.
- Falcao AFD. 2010. Wave energy utilization: a review of the technologies. *Renew Sust Energy Rev.* 14(3):899–918. doi:10.1016/j.rser.2009.11.003.
- Falnes J. 1980. Radiation impedance matrix and optimum power absorption for interacting oscillators in surface waves. *Appl Ocean Res.* 2(2):75–80. doi:10.1016/0141-1187(80)90032-2.
- Falnes J. 2007. A review of wave-energy extraction. *Mar Struct.* 20(4):185–201. doi:10.1016/j.marstruc.2007.09.001.
- GeniE. 2023. Home page of GeniE. Available at: <https://www.dnv.com/services/conceptual-modelling-of-offshore-and-maritime-structures-genie-89128>.
- Giassi M. 2020. Numerical and experimental modelling for wave energy arrays optimization. *Department of electrical engineering.* Uppsala, Sweden: Uppsala University, 85.
- Giassi M, Castellucci V, Götteman M. 2020. Economical layout optimization of wave energy parks clustered in electrical subsystems. *Appl Ocean Res.* 101:102274. doi:10.1016/j.apor.2020.102274.
- Golbaz D, Asadi R, Amini E, et al. 2022. Layout and design optimization of ocean wave energy converters: A scoping review of state-of-the-art canonical, hybrid, cooperative, and combinatorial optimization methods. *Energy Rep.* 8:15446–15479. doi:10.1016/j.egyr.2022.10.403.
- Götteman M, Engström J, Eriksson M, Isberg J. 2014. Methods of reducing power fluctuations in wave energy parks. *J Renew Sustain Energy.* 6(4): 43103 doi:10.1063/1.4889880.
- Götteman M, Giassi M, Engström J, Isberg J. 2020. Advances and challenges in wave energy park optimization—a review. *Front Energy Res.* 8:26. doi:10.3389/fenrg.2020.00026.
- HydroD. 2023. Home page of HydroD. Available at: <https://www.dnv.com/services/hydrodynamic-analysis-and-stability-analysis-software-hydrod-14492>.
- Katsidoniotaki E, Shahroozi Z, Eskilsson C, Palm J, Engström J, Götteman M. 2023. Validation of a CFD model for wave energy system dynamics in extreme waves. *Ocean Eng.* 268:113320. doi:10.1016/j.oceaneng.2022.113320.
- Kuznecovs A, Ringsberg JW, Yang S-H, Johnson E, Andersson A. 2019. A methodology for design and fatigue analysis of power cables for wave energy converters. *Int J Fatigue* 122:61–71. doi:10.1016/j.ijfatigue.2019.01.011.
- Lawson M, Yu Y-H, Ruehl K, Michelén Ströfer CA. 2014. Development and demonstration of the WEC-Sim wave energy converter simulation tool. The 2nd marine energy technology symposium. Seattle, WA.
- Lee H, Poguluri S, Bae Y. 2018. Performance analysis of multiple wave energy converters placed on a floating platform in the frequency domain. *Energies.* 11(2):406. doi:10.3390/en11020406.
- Li X, Xiao Q, Zhou Y, Ning D, Incecik A, Nicoll R, McDonald A, Campbell D. 2022. Coupled CFD-MBD numerical modeling of a mechanically coupled WEC array. *Ocean Eng.* 256:111541. doi:10.1016/j.oceaneng.2022.111541.
- Magkouris A, Bonovas M, Belibassakis K. 2020. Hydrodynamic analysis of surge-type wave energy devices in variable bathymetry by means of BEM. *Fluids.* 5(2):99. doi:10.3390/fluids5020099.
- Oliveira-Pinto S, Rosa-Santos P, Taveira-Pinto F. 2019. Electricity supply to offshore oil and gas platforms from renewable ocean wave energy: Overview and case study analysis. *Energy Convers Manage* 186:556–569. doi:10.1016/j.enconman.2019.02.050.

- Pecher A, Kofoed JP. 2017. Handbook of ocean wave energy. Springer Nature. <https://link.springer.com/book/10.1007/978-3-319-39889-1>
- Raghavan V, Lavidas G, Metrikine A, Mantadakis N, Loukogeorgaki E. 2022. A comparative study on BEM solvers for Wave Energy Converters. *Trends Renew Energ Offshore*. 441–447. doi:10.1201/9781003360773-50.
- Riflex. 2023. Home page of Riflex. Available at: <https://www.dnv.com/services/riser-analysis-software-for-marine-riser-systems-riflex-2312>.
- Ringsberg JW, Jansson H, Örgård M, Yang S-H, Johnson E. 2020a. Design of mooring solutions and array systems for point absorbing wave energy devices—methodology and application. *J Offshore Mech Arct Eng*. 142(3): 31101. doi:10.1115/1.4045370.
- Ringsberg JW, Yang S-H, Lang X, Johnson E, Kamf J. 2020b. Mooring forces in a floating point-absorbing WEC system – a comparison between full-scale measurements and numerical simulations. *Ships Offsh Struct*. 15:S70–S81. doi:10.1080/17445302.2020.1746122.
- Sandberg A, Klemetsen E, Muller G, De Andres A, Maillet J. 2016. Critical factors influencing viability of wave energy converters in off-grid luxury resorts and small utilities. *Sustainability*. 8(12):1274. doi:10.3390/su8121274.
- Sergent P, Baudry V, Bonviller AD, Michard B, Dugor J. 2020. Numerical assessment of onshore wave energy in France: wave energy, conversion and cost. *J Mar Sci Eng*. 8(11):947. doi:10.3390/jmse8110947.
- Shao X. 2023. Analysis of power performance and mooring fatigue damage for wave energy parks. Licentiate Engineering Thesis, Report No. 2023:10. Chalmers University of Technology, Department of Mechanics and Maritime Sciences, Division of Marine Technology, Gothenburg, Sweden.
- Shao X, Ringsberg JW, Yao H-D, Li Z, Johnson E, Fredriksson G. 2023. A comparison of two wave energy converters' power performance and mooring fatigue characteristics – one WEC vs many WECs in a wave park with interaction effects. *J Ocean Eng Sci*. In press. doi:10.1016/j.joes.2023.07.007.
- Sima. 2023. Home page of Sima. Available at: https://www.dnv.com/services/marine-operations-and-mooring-analysis-software-sima-2324?utm_campaign=structure_sesam&utm_source=google&utm_medium=cpc&gad=1&gclid=Cj0KCQjw7uSkBhDGARIsAMCZnJtY8MYtw7vXY5YoQmqO9oDoG2VprKLvJ9YI8NmVtW1oP9domuEFQdkaAm9fEALw_wcB&gclidsrc=a.w.ds.
- Simo. 2023. Home page of Simo. Available at: <https://www.dnv.com/services/complex-multibody-calculations-simo-2311>.
- Stallard T, Stansby PK and Williamson AJ. 2008. An experimental study of closely spaced point absorber arrays. The Eighteenth International Offshore and Polar Engineering Conference. OnePetro, ISOPE-I-08-202.
- Teixeira-Duarte F, Clemente D, Giannini G, Rosa-Santos P, Taveira-Pinto F. 2022. Review on layout optimization strategies of offshore parks for wave energy converters. *Renew Sustain Energy Rev*. 163:112513. doi:10.1016/j.rser.2022.112513.
- Wadam. 2023. Frequency domain hydrodynamic analysis of stationary vessels - Wadam. Available at: <https://www.dnv.com/services/frequency-domain-hydrodynamic-analysis-of-stationary-vessels-wadam-2412>.
- Weller SD, Stallard TJ, Stansby PK. 2010. Experimental measurements of irregular wave interaction factors in closely spaced arrays. *IET Renew Power Gener*. 4(6):628–637. doi:10.1049/iet-rpg.2009.0192.
- Yang B, Wu S, Zhang H, Liu B, Shu H, Shan J, Ren Y, Yao W. 2022. Wave energy converter array layout optimization: a critical and comprehensive overview. *Renew Sustain Energy Rev*. 167:112668. doi:10.1016/j.rser.2022.112668.
- Yang S-H. 2018. Analysis of the fatigue characteristics of mooring lines and power cables for floating wave energy converters. Doctoral (PhD) Thesis, Report No 16:163. Chalmers University of Technology, Department of Shipping and Marine Technology, Division of Marine Technology, Gothenburg, Sweden.
- Yang S-H, Ringsberg JW, Johnson E. 2018. Parametric study of the dynamic motions and mechanical characteristics of power cables for wave energy converters. *J Mar Sci Technol*. 23(1):10–29. doi:10.1007/s00773-017-0451-0.
- Yang S-H, Ringsberg JW, Johnson E. 2020a. Wave energy converters in array configurations—Influence of interaction effects on the power performance and fatigue of mooring lines. *Ocean Eng*. 211:107294. doi:10.1016/j.oceaneng.2020.107294.
- Yang S-H, Ringsberg JW, Johnson E, Hu Z. 2020b. Experimental and numerical investigation of a taut-moored wave energy converter: a validation of simulated mooring line forces. *Ships Offsh Struct*. 15:S55–S69. doi:10.1080/17445302.2020.1772667.